PNAS
www.pnas.org

Supplementary Information for

Endoplasmic reticulum stress leads to accumulation of wild-type SOD1 aggregates associated with sporadic amyotrophic lateral sclerosis

Danilo B. Medinas[a,b,c,1], Pablo Rozas[a,b,c], Francisca Martinez Traub[a,b,c], Ute Woehlbier[a,c,d], Robert H. Brown[e], Daryl A. Bosco[e], and Claudio Hetz[a,b,c,f,g,1]

Claudio Hetz: chetz@med.uchile.cl or chetz@hsph.harvard.edu and Danilo B. Medinas: dmedinas@med.uchile.cl

This PDF file includes:

Supplementary Results
Supplementary Materials and Methods
Figs. S1 to S6
Table S1
References for SI reference citations

www.pnas.org/cgi/doi/10.1073/pnas.1801109115

Supplementary Information Text

Results

ER stress induction *in vivo*

We established a pharmacological paradigm of chronic ER stress in mice by systemic administration of low doses of tunicamycin, an inhibitor of N-glycosylation that causes accumulation of unfolded proteins in the ER lumen. We first confirmed that intraperitoneal injection of tunicamycin causes ER stress in the brain and spinal cord of mice by determining the time-course of UPR activation after administering a high dose of the drug (5 mg/kg body weight) (Fig. S3*B*). Since high doses of tunicamycin injections trigger liver and kidney damage and body weight loss, we optimized dose and schedule of tunicamycin injections for long-term treatment of C57Bl/6 mice. In this manner, we established a paradigm of chronic ER stress induction consisting of subtoxic dosing of tunicamycin (0.1 mg/kg body weight) three times a week over five weeks followed by a last injection 24 h before euthanasia (Fig. 2*B*). This treatment did not significantly alter body weight (Fig. S3*C*). Using this regimen of ER stress stimulation, we determined the levels of UPR activation in spinal cord tissue (Fig. S3*D*) and compared the UPR triggered by chronic and acute ER stress stimulation (Fig. 2*C* and Fig. S3*E*). The UPR under chronic ER stress favored the upregulation of ER chaperones such as ERp57 (Fig. 2*C*), while dictating induction of apoptotic genes such as CHOP upon acute stress (Fig. S3*E*). In addition, we were able to detect the accumulation of HMW poly-ubiquitinated proteins upon tunicamycin administration using the filter-trap assay in wild-type and transgenic animals (Fig. S3*F* and Fig. 2*D*, respectively).

Materials and Methods

Reagents. Tunicamycin was purchased from Calbiochem EMB Biosciences (cat. No. 654380). Antibodies sheep anti-SOD1 from Calbiochem (cat. No. 544597), mouse anti-SOD1 from Pierce (cat. No. LFMA0023), mouse monoclonal anti-SOD1 conformational clones B8H10 and A5C3 from Medimabs (cat. No. MM-0070-P and MM-0070-3, respectively), mouse anti-polyubiquitinated conjugates from Enzo Life Sciences (cat. No. BML-PW8805), mouse anti-β-actin from MP Biomedicals (cat. No. 8691001), mouse anti-α-tubulin from EMD Millipore (cat. No. CP06), rabbit anti-HSP90 from Santa Cruz (cat. No. sc-7947), rabbit anti-TDP-43 from Proteintech (cat. No.10782-2-AP), mouse anti-GFP from Santa Cruz (cat. No. sc-9996), mouse anti-V5 from Invitrogen (cat. No.

R960-25), goat anti-ChAT from EMD Millipore (cat. No. AB144P), rabbit anti-GFAP from abcam (cat. No. ab7260), rabbit anti-Iba1 from Wako (cat. No. 019-19741), mouse anti-PDI from abcam (cat. No. ab2792), mouse anti-ERp57 from abcam (cat. No. ab13506), rabbit anti-ERp72 from Enzo Life Sciences (cat. No. ADI-SPS-720), rabbit anti-calnexin from Enzo Life Sciences (cat. No. ADI-SPA-860), donkey anti-goat biotin-conjugated from Santa Cruz Biotechnology (cat. No. sc-2042), goat anti-rabbit Alexa 568 from Invitrogen (cat. No. A11036), goat anti-rabbit Alexa 488 from Invitrogen (cat. No. A11008), goat anti-mouse HRP-conjugated from Invitrogen (cat. No. 62-6520), goat anti-rabbit HRP-conjugated from Invitrogen (cat. No. 65-6120), donkey anti-sheep HRP-conjugated from Sigma (cat. No. A3415), Protein G-conjugated Sepharose beads from GE Healthcare (cat. No. 17-0618-02), Protein G-conjugated Dynabeads from ThermoFisher Scientific (cat. No.10004D), OxyBlot protein oxidation detection kit from Millipore (cat. No. S7150), Vectastain ABC-HRP kit from Vector Laboratories (PK-6100), TRIzol from Life Technologies (ca. No. 15596018), SuperScriptIII Reverse Transcriptase from Life Technologies (cat. No. 11754250), Primer "Random" for cDNA synthesis from Roche (cat. No 11034731001), HOT FIREPol Eva Green qPCR Mix Plus (ROX) from Solis BioDyne (cat. No. 08-24-00020), GoTag Mix Master Green from Promega (cat. No. M7123), PstI restriction enzyme from New England Biolabs (cat. No. R0140T). Oligonucleotides were manufactured by Integrated DNA Technologies. Cellulose acetate membrane 0.22 µm pore size was from GE Healthcare (cat. No. 10404106). All other reagents were analytical grade or better and obtained from Sigma-Aldrich or Merck.

Transgenic mouse lines. The transgenic mouse lines overexpressing wild-type human SOD1 (hSOD1^{WT}) (B6.Cg-Tg(SOD1)2Gur/J) or the ALS-linked mutant human SOD1^{G93A} (B6.Cg-Tg(SOD1*G93A)1Gur/J) under the control of the endogenous *Sod1* promoter were developed by Gurney and collaborators and purchased from The Jackson Laboratories on a C57BL/6J background (1). The mice were maintained in a 12h dark/light cycle and had *ad libitum* access to food and water. General guidelines for the use of mouse models of ALS were followed as suggested elsewhere (2). The experimental procedures involving these mouse lines were approved by the Institutional Review Board for Animal Care of the Faculty of Medicine of the University of Chile (protocol #0503).

Induction of ER stress *in vivo*. The wild-type human SOD1 transgenic mice (SOD1^{WT}-Tg) and non-transgenic (non-Tg) littermates were submitted to acute and chronic ER

stress paradigms by intraperitoneal administration of tunicamycin, a drug that inhibits N-glycosylation in the endoplasmic reticulum (3). The acute ER stress treatment consisted of a single injection of 5 mg/kg of tunicamycin diluted in sterile solution of 150 mM dextrose followed by euthanasia 24 h later. The chronic ER stress protocol consisted of three weekly injections of 0.1 mg/kg of tunicamycin dilute as above every Monday, Wednesday, and Friday during five weeks followed by a last injection on Monday of the sixth week and euthanasia 24 h after last injection. Control groups received injections of sterile solution of 150 mM dextrose containing the respective amount of DMSO, solvent utilized to prepare concentrated stock solutions of tunicamycin.

Cell Culture, plasmids, transfections, and treatments. The NSC-34 motoneuron-like cell line described in (4) was obtained from Neil Cashman (University of British Columbia, Vancouver, Canada) and cultured in DMEM supplemented with pyruvate, glutamine, 5% fetal bovine serum, and antibiotics (10,000 U/ml Penicillin, 10 µg/ml streptomycin), at 37°C and 5% CO_2. Constructs for expression of C-terminus EGFP-tagged human SOD1 (SOD1-EGFP) and SOD1-EGFP targeted to secretory pathway (ER-SOD1-EGFP) containing superoxide dismutase 3 (SOD3, extracellular SOD) signal peptide in the protein N-terminus were generous gift from Dr. Julie Atkin (Macquarie University, Sydney, Australia) (5). Site-directed mutagenesis to substitute tryptophan-32 for phenylalanine (W32F) in SOD1-EGFP and ER-SOD1-EGFP was performed by Biozilla and confirmed by sequencing (Sacramento, CA, USA). Transient transfections were performed using Effectene (Qiagen) according to manufacturer's instructions. Tunicamycin treatment was performed by addition of 1 µg/ml of the drug to the culture media.

Tissue homogenization and protein extracts. Mouse spinal cord was dissected out by hydraulic extrusion and stored frozen at -80°C until analysis. Human post-mortem spinal cord tissue was received frozen in dry ice and stored at -80°C until analysis. The tissue was homogenized in 400 µl of TEN buffer (10 mM Tris-HCl, 1 mM EDTA, 10 mM NaCl, pH 8.0, containing one cOmplete mini protease inhibitors tablet and one phosphatase inhibitor cocktail PhosSTOP tablet from Roche per 10 ml of buffer) by mechanical disruption using a plastic pestle with snug fit to 1.5 ml plastic tubes on ice. After homogenization, the tissue extract was diluted to different fractions: 1) 50 µl homogenate into 1 ml of TRIzol reagent for RNA extraction, 2) 1:1 dilution of 100 µl homogenate into TEN buffer containing the non-ionic detergent Nonidet P-40 (NP-40) and the thiol

alkylating agent iodoacetamide (0.5% v/v and 50 mM final concentrations, respectively) for analysis of disulfide-dependent HMW protein aggregates, and 3) 1:1 dilution of 250 µl homogenate in TEN buffer containing NP-40 (also to a final concentration of 0.5% v/v) for analysis of total protein, soluble protein fraction, and isolation of detergent-insoluble protein aggregates. The fraction 1) was processed according to TRIzol manufacturer's instructions. The fractions 2) and 3) were sonicated at minimum power for 15s on ice. Cultured cells were recovered with cell scraper, washed with cold PBS, and lysed in TEN buffer containing 0.5% v/v NP-40, 50 mM iodoacetamide, and protease inhibitor cocktail (cOmplete, Roche) with sonication at minimum power for 15s on ice. Protein concentration was determined by the Pierce BCA Protein Assay kit from ThermoFisher Scientific (cat. No. 23225).

Quantitative real-time PCR analysis. cDNA was synthetized using SuperScriptIII following manufacturer's instructions (Life Technologies, 11754250). Quantitative real-time PCR was performed using HOT FIREPol Eva Green qPCR Mix Plus (ROX) (Solis BioDyne, 08-24-00020). Actin was employed as housekeeping control. Primer sequences: Xbp1s: forward 5'-TGCTGAGTCCGC-AGCAGGTG-3' and reverse 5'-GACTAGCAGACT-CTGGGGAAG-3'; Bip: forward 5'-TCATCGGACGCACTTGGAA-3' and reverse 5'- CAACCACCTTGAATGGCAAGA-3'; Edem1: forward 5'-AAGCCCTCTGGAACTTGCG-3' and reverse 5'-AACCCAATGGCCTGTCTGG-3'; Chop: forward 5'-GTCCCTAGCTTGGCTGACAGA-3' and reverse 5'-TGGAGAGCGAGGGCTTTG'; Erp57: forward 5'-GAGGCTTGCCCCTGAGTATG-3' and reverse 5'-GTTGGCAGTGCAATCCACC-3'; Actin: forward 5'-CTCAGGAGGAGCAATGATCTTGAT-3' and reverse 5'-TACCACCATGTACCCAGGCA-3'. Splicing of XBP1 mRNA was also evaluated by conventional PCR using the primers Xbp1: forward 5'-AAACAGAGTAGCAGCGCAGACTGC-3' and reverse 5'-GGATCTCTAAAACTAGAGGCTTGGTG-3' followed by digestion with the restriction enzyme PstI as previously described (6).

Analysis of disulfide-dependent HMW protein aggregates. Protein extracts alkylated with iodoacetamide were treated or not with 100 mM of the thiol reducing agent dithiothreitol (DTT) in TEN buffer supplemented with 50 mM Tris-HCl pH 8.0 for 30 min on ice, and then diluted in PBS containing 1% w/v sodium dodecyl sulfate (SDS) for filter-trap analysis (7, 8). Shortly, samples are filtered through 0.22 µm acetate cellulose membrane under vacuum using a dot-blot apparatus. After filtration, membranes are

washed during 15 min with PBS containing 1% w/v SDS and then processed using standard protocols for immunodetection of protein aggregates trapped in the membrane pores. To ascertain the percentage of sALS patients (and controls) containing relevant amount of SOD1 aggregates, we established a cut-off criteria considering positive cases as those presenting relative intensities equal to or above the mean value of the sALS group.

For western blot analysis, samples were diluted in Laemmli's loading buffer in the absence or presence of 100 mM of DTT and incubated 5 min at 95°C. Then, the samples under non-reducing and reducing conditions were run separately on SDS-PAGE mini gels at 80 V. Before electroblotting of proteins on PVDF membranes, the gels were incubated for 30 min in SDS-PAGE running buffer containing 50 mM DTT under gentle agitation to assure even transfer of disulfide reduced and oxidized proteins. Membranes were then submitted to typical western blot procedures.

Isolation of detergent-insoluble protein aggregates. The fraction 3 described above was cleared through three cycles of centrifugation at 4°C, 1,000*g* for 10 min each. The supernatant was then submitted to centrifugation at 4°C, 16,900*g* for 45 min for separation of the soluble protein fraction and the detergent-insoluble protein aggregates (9–11). The soluble protein fraction was transferred to a new tube, and the pellet containing aggregates washed by addition of TEN buffer (containing 0.5% NP-40 and protease inhibitors) with sonication at minimum power for 15s on ice. The resuspended pellet was then centrifuged at 4°C, 1,000*g* for 10 min to sediment remaining debris followed by centrifugation of the cleared supernatant at 4°C, 16,900*g* for 45 min to sediment protein aggregates. The detergent-insoluble aggregates were submitted to three washing cycles to yield a translucent pellet that was solubilized in TEN buffer containing 0.25% SDS and 0.5% sodium deoxycholate followed by western blot analysis under reducing conditions.

Analysis of soluble misfolded human SOD1. The soluble protein fraction obtained during isolation of detergent-insoluble aggregates was employed for analysis of soluble misfolded human SOD1 using immunoprecipitation with conformation-specific antibodies to human SOD1. Thus, the soluble fraction was diluted to 1 mg protein/ml and submitted to a pre-clearing step with 30 µl of Protein G-conjugated Sepharose beads for 2 h under rotation at 4°C. The conformation-specific antibody to human SOD1 clone B8H10 was selected since it resulted to be more efficient and specific in immunoprecipitation assays.

The Protein G-conjugated Sepharose beads were first blocked with bovine serum albumin (BSA) followed by antibody binding for 4 h under rotation at 4°C. The complex antibody-Protein G-conjugated Sepharose beads (0.25 µg antibody/30 µl beads) was then incubated with 1 ml of the pre-cleared soluble extract overnight under rotation at 4°C. Finally, the beads were extensively washed with high-salt TEN (containing 500 mM NaCl), resuspended in 50 µl Laemmli's loading buffer, and analyzed by western blot.

Detection of oxidized proteins. Protein oxidation was measured using the OxyBlot kit to detect carbonylation according to manufacturer's instructions (Millipore, cat. No. S7150).

Subcellular fractionation by differential centrifugation. Freshly harvested mouse spinal cord was homogenized in lysis buffer (50 mM HEPES, 250 mM sucrose, 1 mM $MgCl_2$, 50 mM iodoacetamide, pH 7.4 containing protease and phosphatase inhibitors cocktail) using a Dounce tissue grinder with 0.0013 mm of clearance. The homogenate was centrifuged twice at 4°C, 1,000*g* for 10 min to yield nucleus-enriched P1 pellet and S1 supernatant. The P1 pellet was washed twice in lysis buffer. The S1 supernatant was centrifuged twice at 4°C, 10,000*g* for 30 min to yield mitochondria-enriched P2 pellet and S2 supernatant. The P2 pellet was washed twice in lysis buffer. The S2 supernatant was centrifuged at 4°C, 100,000*g* for 1 h to yield microsomal P3 pellet (ER-enriched) and S3 supernatant (cytosol-enriched). The P3 pellet was washed once in lysis buffer. All samples were stored frozen at -80°C until analysis.

For filter-trap and western blot analysis, the pellet fractions were solubilized in TEN buffer containing 0.5% v/v NP-40, 0.25% w/v SDS, and protease and phosphatase inhibitors cocktail, with sonication at minimum power for 15s on ice. For mass spectrometry analysis, the pellet fractions were solubilized in TEN buffer containing 0.2% v/v NP-40 and protease and phosphatase inhibitors cocktail, with sonication at minimum power for 15s on ice. Protein concentration was determined by the Pierce BCA Protein Assay kit as above.

Histological analysis. Mice were perfused with cold saline followed by 4% w/v paraformaldehyde in PBS (4% PFA) and spinal cord dissected out by laminectomy. The tissue was cut into lumbar, thoracic, and cervical segments and post-fixed overnight in 4% PFA at 4°C. The fixed tissue was then cryoprotected in 30% w/v sucrose in PBS, embedded in freezing media (O.C.T., Tissue-Tek), and frozen in liquid nitrogen. The lumbar spinal cord was cryosectioned into 25 µm sections collected free-floating in 96-

well plates (1 section per well) and stored in PBS containing 0.1% w/v sodium azide at 4°C until analysis.

Sixteen serial sections spaced every 200 μm were employed for immunohistochemical staining of motoneurons using goat anti-choline acetyltransferase (anti-ChAT, EMD Millipore, cat. No. AB144P) as we recently described (12). Briefly, spinal cord tissue was submitted to antigen-retrieval in citrate buffer for 15 min at 95°C, treated with 3% v/v hydrogen peroxide for 30 min for inactivation of endogenous peroxidases, mounted on glass slides, blocked with 3% w/v bovine serum albumin (3% BSA) and 10% v/v normal goat serum (10% NGS) in PBS containing 0.1% v/v Triton X-100, incubated with 1:250 dilution of anti-ChAT in blocking buffer for 48 h at room temperature, incubated with 1:500 dilution of donkey anti-goat biotin-conjugated followed by avidin/biotin-HRP (ABC kit, Vector Laboratories) for 2 h, developed with 3,3'-diaminobenzidine (DAB), and finally mounted with Entellan (EMD Millipore). Microphotographs were acquired in bright field using the Tissue Scanner NanoZoomer XR (Hamamatsu Photonics K.K. Japan). Staining and motoneuron counting were performed by a blinded observer to treatments and genotypes.

For staining of astrocytes and microglia, we performed immunofluorescence against rabbit anti-glial fibrillary acidic protein (anti-GFAP, abcam, cat. No. ab7260) and rabbit anti-ionized calcium-binding adapter molecule 1 (anti-Iba1, Wako, cat. No. 019-19741), respectively. Shortly, four serial sections spaced every 800 μm were mounted on glass slides, blocked with 3% BSA and 10% NGS in PBS containing 0.1% v/v Triton X-100, incubated with 1:500 dilution of anti-GFAP or 1:250 anti-Iba1 in blocking buffer overnight at room temperature, incubated with 1:1000 dilution of fluorescent Alexa-conjugated secondary antibody, and finally mounted with Fluoromount containing DAPI. Microphotographs were taken using a C2+ confocal microscope using 40x objective (Nikon, Japan). Staining and quantification of astrocytes and microglia were performed by a blinded observer to treatments and genotypes. Area coverage of GFAP and Iba1 staining in the grey matter was quantified using ImageJ and expressed as GFAP and Iba1 burden, respectively.

Mass spectrometry determination of SOD1 posttranslational modifications. The solubilized P2 and P3 pellets and S3 supernatant were diluted in PBS-T (PBS with 0.1% v/v Tween-20) to 1 mg protein/ml. Seven animals were pooled per sample. The mouse anti-SOD1 antibody from Pierce (cat. No. LFMA0023) was bound to Protein G-

conjugated Dynabeads according to manufacturer's instructions (10 μg antibody/50 μl beads) and then added to samples for immunoprecipitation of SOD1 for 2 h under rotation at room temperature. The magnetic beads were washed extensively with PBS-T and then transferred to a new tube. SOD1 was eluted from the beads by incubation with reducing Laemmli's loading buffer at 37°C for 10 min and subjected to SDS-PAGE. Coomassie blue-stained SOD1 bands were excised with a scalpel, cut into 1 mm2 pieces, and submitted to *in-gel* digestion with trypsin (Promega, cat. No. V5111) as described elsewhere (13).

Extracted peptides were lyophilized and resuspended in 5% acetonitrile with 0.1% trifluroacetic acid immediately prior to injection on LC/MS/MS. The peptides were separated by liquid chromatography using a 2 cm x 100 μm C18 Magic 5 μm particle trap column and sprayed from a custom packed emitter (75 μm x 25 cm C18 Magic 3 μm particle) with a linear gradient from 95% solvent A (0.1% formic acid in water) to 35% solvent B (0.1% formic acid in acetonitrile) in 45 minutes at a flow rate of 300 nanoliters per minute on a Waters Nano Acquity UPLC system. Data dependent acquisitions were performed on a Q Exactive mass spectrometer (Thermo Scientific) according to an experiment where full MS scans from 300-1750 m/z were acquired at a resolution of 70,000 followed by 10 MS/MS scans acquired under HCD fragmentation at a resolution of 17,500 with an isolation width of 1.6 Da. Raw data files were processed with Proteome Discoverer (version 1.4) with Mascot (Version 2.5, Matrix Science) using the human Uniprot database. An error tolerant search was employed to identify modifications present on SOD1 peptides. Scaffold (Proteome Software, Inc.) and Skyline (MacCoss Lab Software) software were used to quantify the modified (oxidation, deamidation, carbamidomethylation, N-term acetylation, phosphorylation) and unmodified peptides (false discovery rate (FDR), 1.3%) identified in the error tolerant search (14).

Statistical analysis. Statistics were performed using Prism 6.0 (GraphPad Software). Details are indicated in legends to figures.

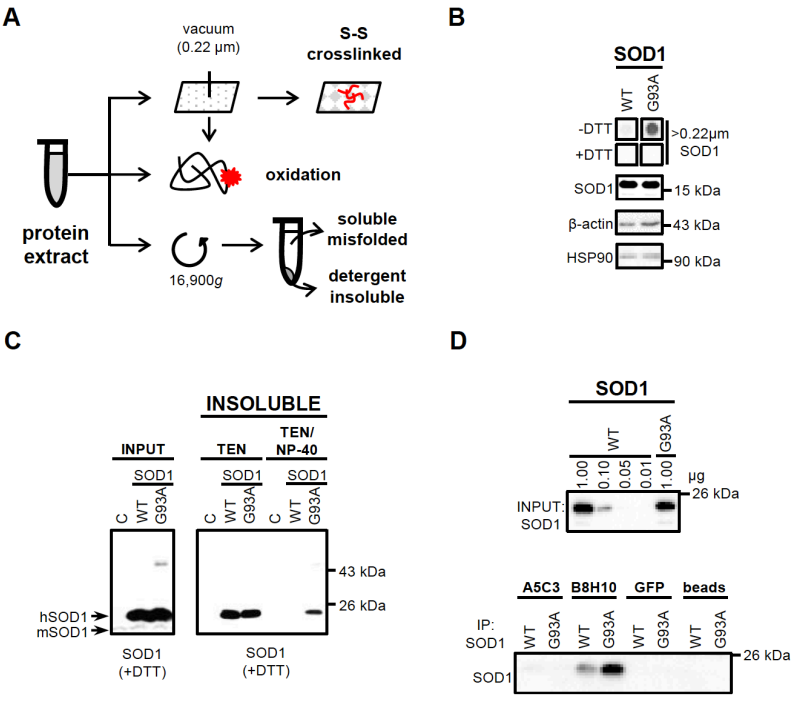

Fig. S1. Biochemical methods used to study SOD1^{WT} misfolding and aggregation. (*A*) Experimental workflow for analysis of abnormal SOD1^{WT} species. Total extracts can be directly analyzed by filter-trap and western blot for detection of HMW SOD1 aggregates and oxidized SOD1, respectively. The centrifugal sedimentation in the presence of non-ionic detergent (NP-40) yields a pellet of protein aggregates and a supernatant fraction containing soluble misfolded SOD1 species that can be detected by immunoprecipitation with conformation-specific antibodies. (*B*) Filter-trap assay for detection of HMW SOD1 aggregates under non-reducing (-DTT) and reducing (+DTT) conditions. Comparison of SOD1 aggregates in total spinal cord extracts of a transgenic mouse overexpressing SOD1^{WT} (SOD1^{WT}-Tg) and a symptomatic transgenic mouse overexpressing SOD1^{G93A} (SOD1^{G93A}-Tg). (*C*) Western blot analysis of centrifugal sedimentation pellet obtained from spinal cord extract of SOD1^{WT}-Tg and symptomatic SOD1^{G93A}-Tg mice with and without addition of non-ionic detergent (NP-40). Lane labelled C, non-Tg control. (*D*) Immunoprecipitation of SOD1 from spinal cord soluble fraction of SOD1^{WT}-Tg and symptomatic SOD1^{G93A}-Tg mice using two different conformation-specific antibodies to SOD1 and control incubations with unrelated antibody (anti-GFP, same IgG isotype) or Protein-G Sepharose beads only.

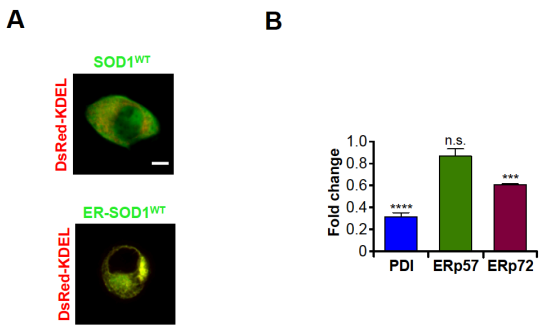

Fig. S2. Overexpression of ER-SOD1^{WT} construct in NSC-34 cells. (*A*) NSC-34 cells were transiently co-transfected with constructs for overexpression of SOD1^{WT}-EGFP or ER-SOD1^{WT}-EGFP containing SOD3 (extracellular SOD)-signal peptide (ER-targeting sequence) and KDEL-DsRed to stain the ER. Microphotographs show representative live cells 48 h after transfection (scale bar, 5 μm). (*B*) NSC-34 cells were transiently co-transfected with constructs for overexpression of ER-SOD1^{WT}-EGFP and the indicated PDI family member or empty vector (mock). Graph shows quantification of disulfide-dependent SOD1 aggregates in each condition relative to mock. Statistical analysis was performed using one-way ANOVA with Tukey's multiple comparison test. Mean ± S.E. is shown; p values are as follows: n.s., $p > 0.05$; ***, $p \leq 0.001$; ****, $p \leq 0.0001$. n = 3.

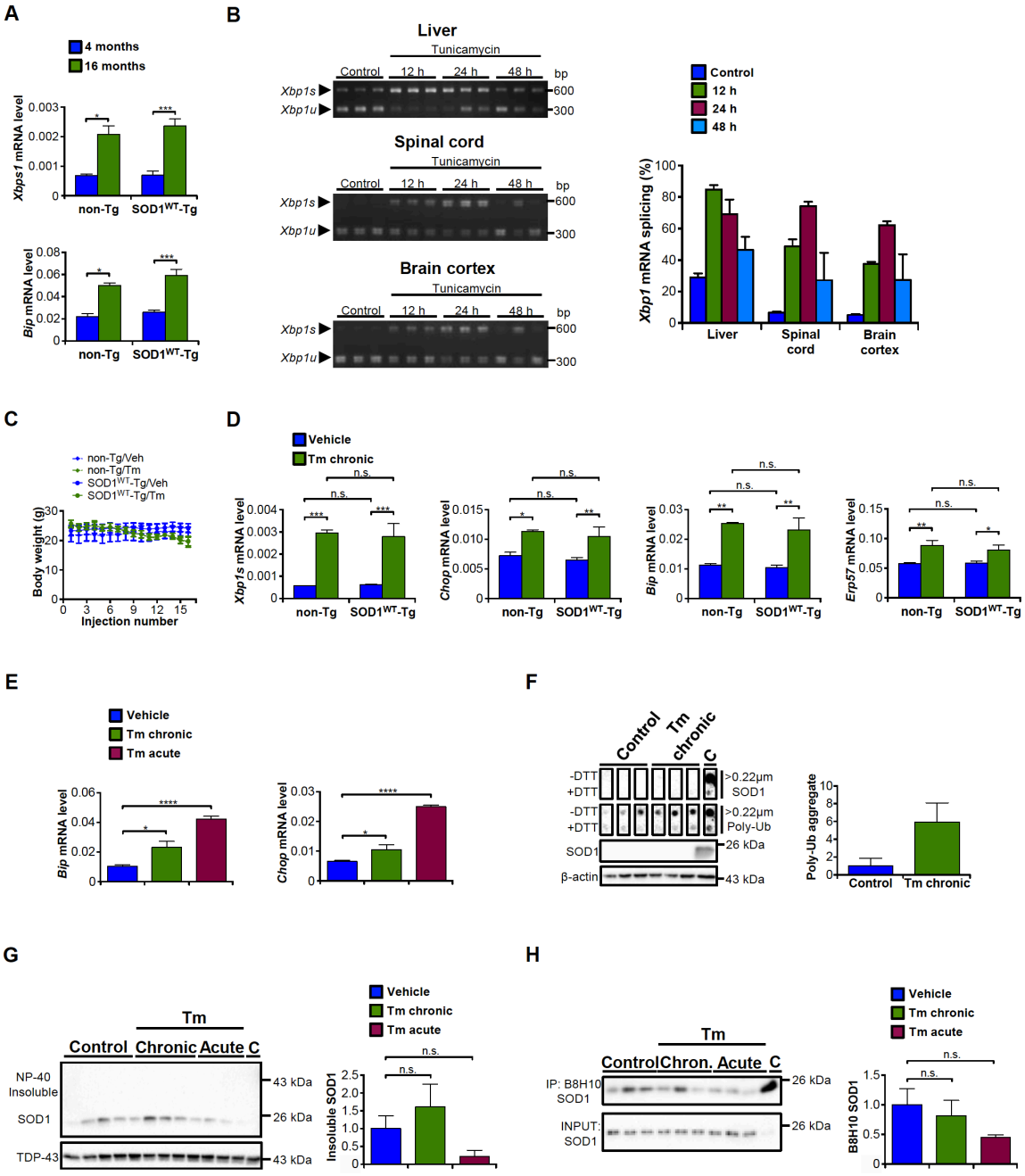

Fig. S3. Models of ER stress *in vivo*. (*A*) mRNA levels of the ER stress marker Xbp1s and ER chaperone Bip were analyzed by quantitative PCR in the spinal cord tissue of transgenic mice overexpressing SOD1^{WT} (SOD1^{WT}-Tg) and non-transgenic littermates (non-Tg) at different ages (n = 3-6 per group). (*B*) Wild-type mice were treated with a single high-dose intraperitoneal injection of tunicamycin (Tm, 5 mg/kg) for different periods of time. The kinetics of XBP1 splicing was measured in liver, spinal cord, and brain cortex using conventional PCR. (*C*) Body weight curve of SOD1^{WT}-Tg and non-Tg

mice treated with 0.1 mg/kg i.p. injections of Tm for induction of chronic ER stress. (*D*) $SOD1^{WT}$-Tg mice and non-Tg littermates were subjected to chronic Tm treatment and ER stress markers measured by quantitative PCR in spinal cord tissue. (*E*) mRNA levels of the ER stress marker Chop and Bip were analyzed by quantitative PCR in the spinal cord tissue of $SOD1^{WT}$-Tg mice submitted to chronic or acute Tm treatments as described in Figure 2. (*F*) Filter-trap assay under non-reducing (-DTT) and reducing (+DTT) conditions for detection of HMW SOD1 and Poly-ubiquitinated aggregates in spinal cord tissue of non-Tg mice receiving chronic Tm treatment. A symptomatic transgenic mouse overexpressing $SOD1^{G93A}$ mutant ($SOD1^{G93A}$-Tg) was used as positive control for aggregate detection (lane labelled C). (*G*) Western blot analysis of non-ionic detergent (NP-40)-insoluble SOD1 aggregates isolated by centrifugal sedimentation from spinal cord of $SOD1^{WT}$-Tg mice submitted to chronic or acute Tm treatments as described in Figure 2. TDP-43 was used as loading control of detergent-insoluble fraction. A non-Tg littermate was used as technical control for background signal (lane labelled C). (*H*) Immunoprecipitation with SOD1 conformation-specific antibody (clone B8H10) was performed in soluble fractions of spinal cord (supernatant of 16,900*g*) of $SOD1^{WT}$-Tg mice submitted to chronic or acute Tm treatments as described in Figure 2 and analyzed by western blot. SOD1 in the input was used as loading control. A symptomatic transgenic mouse overexpressing mutant $SOD1^{G93A}$ was used as positive control for immunoprecipitation (lane labelled C). Statistical analysis was performed using two-way ANOVA (A, C and D) or one-way ANOVA (E, G and H) with Tukey's multiple comparison test. Mean ± S.E. is shown; p values are as follows: n.s., $p > 0.05$; *, $p \leq 0.05$; **, $p \leq 0.01$; ***, $p \leq 0.001$. n = 3-6 per group.

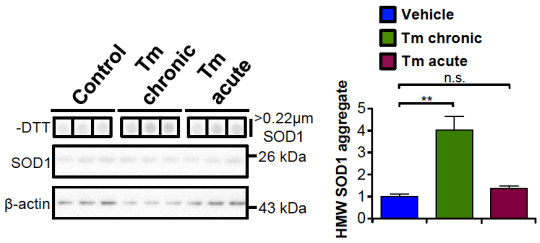

Fig. S4. Accumulation of SOD1^{WT} aggregates in aged mice subjected to chronic ER stress. Filter-trap assay under non-reducing (-DTT) conditions for detection of HMW SOD1 aggregates in total spinal cord extracts of aged (16-month-old) SOD1^{WT}-Tg mice submitted to chronic ER stress protocol. β-actin was employed as loading control. Statistical analysis was performed using one-way ANOVA with Tukey's multiple comparison test. Mean ± S.E. is shown; p values are as follows: n.s., $p > 0.05$; **, $p \leq 0.01$. n = 3 per group.

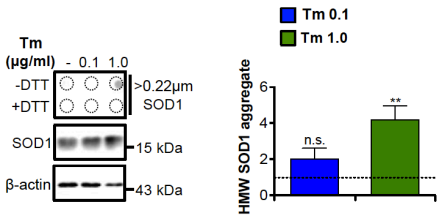

Fig. S5. Disulfide-dependent aggregation of endogenous SOD1 in NSC34 cell line under ER stress. NSC34 cells were treated with the indicated concentrations of tunicamycin added to the culture media for 24 h and analyzed by filter-trap for detection of SOD1 aggregates. β-actin was employed as loading control. Graph shows quantification of fold change to control group treated with vehicle. Statistical analysis was performed using one-way ANOVA with Tukey's multiple comparison test. Mean ± S.E. is shown; *p* values are as follows: n.s., $p > 0.05$; **, $p \leq 0.01$. n = 4 per group.

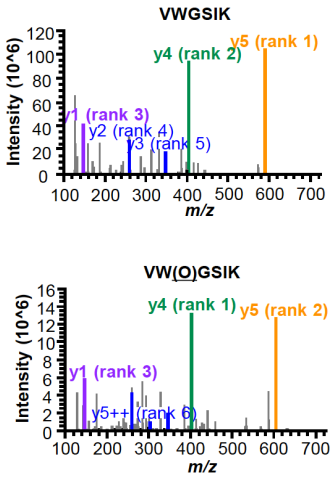

Fig. S6. Detection of oxidized tryptophan-32 of human SOD1^{WT} by mass spectrometry. MS/MS spectra of SOD1 tryptic peptide containing unmodified (upper panel, VWGSIK, m/z = 345.20 2+) or oxidized (lower panel, VW(O)GSIK, m/z = 353.20 2+) tryptophan-32.

Additional data Table S1

Table S1. Clinical and histopathological data of control and sporadic ALS cases.

Case	Age	Sex	Diagnosis	Spinal cord tissue	Neuropathology/others	Disease duration (yrs)
1	57	M	sALS	cervical, thoracic, lumbar	TDP-43 inclusions in spinal cord	4
2	59	F	sALS	cervical, thoracic, lumbar	Ubiquitin and TDP-43 inclusions in motoneurons of precentral gyrus and ventral horn	2
3	59	F	sALS	cervical, thoracic, lumbar	TDP-43 inclusions in anterior horn cells	N.A.
4	60	M	sALS	cervical, thoracic, lumbar	TDP-43 inclusions in primary motor/sensory cortex and spinal cord	2
5	64	F	sALS	cervical, thoracic, lumbar	No TDP-43 or ubiquitin positive inclusions	5
6	65	M	sALS	cervical, thoracic, lumbar	TDP-43 inclusions in spinal cord	3
7	66	M	sALS	cervical, thoracic, lumbar	No TDP-43 or ubiquitin positive inclusions	N.A.
8	81	M	sALS	cervical, thoracic, lumbar	No inclusions seen in primary motor/sensory cortex or spinal cord	1
9	58	F	control	cervical, thoracic, lumbar		
10	82	M	control	cervical, thoracic		
11	34	M	control	lumbar	coronary atherosclerosis	
12	65	M	control	lumbar		
13	80	F	control	lumbar		
14	80	M	control	lumbar		
15	57	M	control	lumbar	familial history of dementia	

N.A. = not available

References

1. Gurney ME, et al. (1994) Motor neuron degeneration in mice that express a human Cu,Zn superoxide dismutase mutation. *Science* 264(5166):1772–5.

2. Ludolph AC, et al. (2010) Guidelines for preclinical animal research in ALS/MND: A consensus meeting. *Amyotroph Lateral Scler* 11(1–2):38–45.

3. Esko JD, Bertozzi CR (2009) *Chemical Tools for Inhibiting Glycosylation* Available at: http://www.ncbi.nlm.nih.gov/pubmed/20301258.

4. Cashman NR, et al. (1992) Neuroblastoma x spinal cord (NSC) hybrid cell lines resemble developing motor neurons. *Dev Dyn* 194(3):209–21.

5. Turner BJ, et al. (2005) Impaired extracellular secretion of mutant superoxide dismutase 1 associates with neurotoxicity in familial amyotrophic lateral sclerosis. *J Neurosci* 25(1):108–17.

6. Hetz C, et al. (2009) XBP-1 deficiency in the nervous system protects against amyotrophic lateral sclerosis by increasing autophagy. *Genes Dev* 23(19):2294–306.

7. Scherzinger E, et al. (1997) Huntingtin-encoded polyglutamine expansions form amyloid-like protein aggregates in vitro and in vivo. *Cell* 90(3):549–58.

8. Wanker EE, et al. (1999) Membrane filter assay for detection of amyloid-like polyglutamine-containing protein aggregates. *Methods Enzymol* 309:375–86.

9. Wang J, Xu G, Borchelt DR (2006) Mapping superoxide dismutase 1 domains of non-native interaction: roles of intra- and intermolecular disulfide bonding in aggregation. *J Neurochem* 96(5):1277–88.

10. Wang J, et al. (2003) Copper-binding-site-null SOD1 causes ALS in transgenic mice: aggregates of non-native SOD1 delineate a common feature. *Hum Mol Genet* 12(21):2753–64.

11. Jonsson PA, et al. (2006) Disulphide-reduced superoxide dismutase-1 in CNS of transgenic amyotrophic lateral sclerosis models. *Brain* 129(Pt 2):451–64.

12. Bargsted L, et al. (2017) Disulfide cross-linked multimers of TDP-43 and spinal motoneuron loss in a TDP-43(A315T) ALS/FTD mouse model. *Sci Rep* 7(1):14266.

13. Shevchenko A, Tomas H, Havli\[sbreve] J, Olsen J V, Mann M (2007) In-gel digestion for mass spectrometric characterization of proteins and proteomes. *Nat Protoc* 1(6):2856–2860.

14. MacLean B, et al. (2010) Skyline: an open source document editor for creating and analyzing targeted proteomics experiments. *Bioinformatics* 26(7):966–8.